AMERICAN JOURNAL OF PHYSIOLOGY
LUNG CELLULAR AND MOLECULAR PHYSIOLOGY

Am J Physiol Lung Cell Mol Physiol 328: L603–L615, 2025.
First published March 24, 2025; doi:10.1152/ajplung.00409.2024

RESEARCH ARTICLE

Women's Health Research and Pregnancy, Postnatal Conditions, Endometriosis, Polycystic Ovarian Syndrome, Preeclampsia

Intraamniotic vitamin D preserves lung development and prevents pulmonary hypertension in experimental bronchopulmonary dysplasia due to intraamniotic sFlt-1

Michael W. Cookson,[1,2] Tania Gonzalez,[1,2] Elisa M. Bye,[1,2] Greg Seedorf,[1,2,3] Sarah Ellor,[1,2] Bradford J. Smith,[1,4] James C. Fleet,[5] and Erica W. Mandell[1,2]

[1]*Section of Neonatology, Department of Pediatrics, University of Colorado, Anschutz School of Medicine and Children's Hospital Colorado, Aurora, Colorado, United States;* [2]*Pediatric Heart Lung Center, Department of Pediatrics, University of Colorado, Anschutz School of Medicine, Aurora, Colorado, United States;* [3]*Section of Pulmonary and Sleep Medicine, Department of Pediatrics, University of Colorado, Anschutz School of Medicine and Children's Hospital Colorado, Aurora, Colorado, United States;* [4]*Department of Bioengineering, College of Engineering and Applied Sciences, University of Colorado Denver, Anschutz Medical Campus, Aurora, Colorado, United States; and* [5]*Department of Nutritional Sciences, University of Texas, Austin, Texas, United States*

Abstract

Preterm infants born to mothers with preeclampsia, a disease of vascular dysfunction, are at increased risk for bronchopulmonary dysplasia (BPD). Endothelial cells are critical in both maintaining proper vascular function and coordinating lung development. Understanding the mechanisms contributing to BPD in the setting of preeclampsia and how preeclampsia impacts pulmonary endothelial cells (PECs) in the newborn lung are required to decrease the burden of BPD. Vitamin D has been shown to improve lung angiogenesis and lung development in inflammatory models of BPD, but its therapeutic potential in the setting of preeclampsia is unknown. We hypothesized that intraamniotic (IA) treatment with the biologically active form of vitamin D, 1,25 dihydroxyvitamin D [1,25$(OH)_2$D], will preserve lung growth in an experimental model of BPD induced by antenatal exposure to soluble vascular endothelial growth factor receptor-1 [sFlt-1 (soluble fms-like tyrosine kinase 1)]. Fetal rats were exposed to saline (control), sFlt-1 alone, 1,25$(OH)_2$D alone, or simultaneous sFlt-1 + 1,25$(OH)_2$D via IA injection during the late canalicular stage of lung development and delivered 2 days later. IA treatment with 1,25$(OH)_2$D in sFlt-1-exposed pups improved lung alveolar and vascular growth and function at 14 days of life. PECs orchestrate alveolar development, and we demonstrate that IA sFlt-1 exposure alone decreased in vitro growth and tube formation of PECs isolated from newborn pups and that PECs from pups coexposed to IA sFlt-1 and 1,25$(OH)_2$D demonstrated increased growth and tube formation. We conclude that IA 1,25$(OH)_2$D treatment improves distal lung development during sFlt-1 exposure through preservation of angiogenesis in the developing lung.

NEW & NOTEWORTHY This study highlights that experimental BPD induced by intraamniotic sFlt-1 is associated with impaired growth in postnatal pulmonary endothelial cells. We demonstrate that 1,25$(OH)_2$D may be a therapeutic option to improve lung development through enhancement of VEGF signaling and preservation of early pulmonary endothelial growth in the newborn rat lung.

bronchopulmonary dysplasia; neonatal lung development; preeclampsia; pulmonary endothelial cells; vitamin D

INTRODUCTION

Bronchopulmonary dysplasia (BPD) is the chronic lung disease of infancy that complicates the clinical course and outcomes of preterm newborns (1–4). The incidence of BPD remains over 40% in preterm infants born before 28 wk gestation, with increasing incidence and severity as gestational age at birth decreases (5, 6). Infants diagnosed with severe BPD are at high risk for death, pulmonary hypertension, frequent respiratory infections, persistent abnormal lung function, exercise intolerance, and late neurodevelopmental sequelae (7–10). BPD is characterized by a disruption of distal lung growth with impaired alveologenesis and angiogenesis, but mechanisms that cause

Correspondence: M. W. Cookson (Michael.cookson@cuanschutz.edu).
Submitted 16 December 2024 / Revised 10 January 2025 / Accepted 12 March 2025

sustained abnormalities of lung structure are poorly understood (4, 11).

Past studies have shown that early lung injury reduces angiogenesis, which impairs alveolarization through disruption of endothelial-epithelial cross talk or "angiocrine" signaling (the "vascular hypothesis" of BPD) (12). Preclinical and clinical studies have shown that early postnatal disruption of proangiogenic pathways, such as vascular endothelial growth factor (VEGF) signaling, plays a critical role in the pathogenesis of BPD (13–15). However, mechanisms that disrupt angiogenesis in the developing lung and therapeutic strategies to preserve proangiogenic signaling in infants at risk for BPD remain elusive, making it challenging to develop effective therapies.

Preeclampsia is a vascular disorder of pregnancy associated with an abnormal intrauterine environment marked by elevations in antiangiogenic peptides (16–18). Although postnatal exposures increase the risk for the development of BPD, gestational pathologies, such as preeclampsia, increase the risk of developing BPD (19–22). Recent studies have demonstrated that placental histologic and biomarkers of vascular maldevelopment, which are common in preeclampsia, are associated with the subsequent development of BPD (23, 24). Increased levels of soluble VEGF receptor-1 [sFlt-1 (soluble fms-like tyrosine kinase 1)], an endogenous VEGF inhibitor, is elevated in maternal blood and amniotic fluid preceding the development of preeclampsia (25, 26). Increased sFlt-1 and decreased VEGF levels in tracheal fluid from preterm infants are further associated with the development of BPD, suggesting that imbalances in angiogenic signaling at the fetal-maternal interface persist after birth and contribute to neonatal pulmonary vascular disease (27). Rodent models of preeclampsia-related BPD demonstrated that antenatal exposure to sFlt-1 decreases alveolar and pulmonary vascular growth and causes right ventricular hypertrophy (RVH); however, there exists an ongoing need to develop therapies to preserve lung development (28, 29).

Although vitamin D is a well-described steroid hormone central to calcium and bone homeostasis, vitamin D has many other physiologic roles, including regulation of the developing lung (30, 31). Vitamin D signaling occurs through the vitamin D receptor (VDR), which is ubiquitously expressed in tissues, including in the early lung (32–36). Vitamin D plays a role in the maturation of multiple resident lung cell types, including epithelial, fibroblast, and mesenchymal lineages (37–40). The specific role of vitamin D in supporting resident lung endothelial cell health continues to be investigated. 1,25 Dihydroxyvitamin D [1,25$(OH)_2$D], the biologically active metabolite of vitamin D, has been shown to increase in vivo VEGF expression in the developing rodent lung and increase in vitro growth of pulmonary artery endothelial cells (41, 42). Previous work from our laboratory has demonstrated that intraamniotic (IA) therapy with 1,25$(OH)_2$D improves placental vascular development, improves alveolarization, and prevents RVH in a rat model of chorioamnionitis induced BPD (42–44). IA therapy carries significant limitations clinically; however, the use of IA 1,25$(OH)_2$D allows for the exploration of potential mechanisms affecting early neonatal lung development. Whether IA 1,25$(OH)_2$D treatment can attenuate sFlt-1-induced lung injury in experimental BPD is unknown; therefore, we hypothesized that IA 1,25$(OH)_2$D treatment will prevent IA sFlt-1 induced lung injury and prevent RVH in a rat model of preeclampsia related BPD.

METHODS

Animal Model and Study Design

All procedures and protocols were approved by the Animal Care and Use Committee at the University of Colorado Health Sciences Center. Timed pregnant Sprague-Dawley Crl:(SD)BR rats (Charles River Laboratories) were used for all experiments. Animals underwent intraamniotic injections using standard methods, as previously described (28, 29, 43). Briefly, a laparotomy was performed at 20 days of gestation (term: 22 days), corresponding to the late canalicular stage of lung development in the rat, and intraamniotic (IA) injections were performed. Pregnant rats were randomly assigned to 1 of 4 groups: *1*) control group, 50 μL of normal saline/amniotic sac; *2*) sFlt-1 group, 1 μg of recombinant human sFlt-1 (R&D Systems) diluted in 50 μ saline/amniotic sac; *3*) 1,25$(OH)_2$D group, 50 pg of 1,25$(OH)_2$D diluted in 50 μL saline/amniotic sac; and *4*) sFlt-1 + 1,25$(OH)_2$D group, 1 μg of recombinant human sFlt-1 plus 50 pg of 1,25$(OH)_2$D (Cayman Chemical) diluted in 50 μL saline/amniotic sac (28, 29, 42–44).

Pregnant rats were recovered and observed for 2 days following study administration. At gestational day 22 (full-term), a cesarean section was performed on pregnant rats under general anesthesia with isoflurane inhalation. All rat pups in the injected amniotic sacs were delivered within 5 min after onset of anesthesia. Dams were then euthanized with pentobarbital sodium. Pups were cross fostered with a dam that delivered a spontaneous litter of pups at the same time as the experimental pups were delivered.

Tissue for Histological Analysis

Animals were euthanized at 14 days of life with intraperitoneal pentobarbital sodium. The thorax was opened, and the lungs were inflated to 20 cmH_2O for 60 min with 4% paraformaldehyde via a tracheal catheter. A ligature was tightened around the trachea to maintain pressure as the tracheal cannula was removed. Lungs were immersed in 4% paraformaldehyde at room temperature for at least 24 h for fixation. Two mm thick transverse sections were taken from the midplane of the left lobe of the fixed lungs for processing and paraffin embedding.

Immunohistochemistry

Slides with 5 μm paraffin sections were stained with hematoxylin and eosin for assessing alveolar structures. Immunostaining was completed with von Willebrand Factor (vWF), an endothelial cell-specific marker (Table 1) [primary Dako vWF-8, Cat. No. A0082 at 1:1,000 dilution, secondary biotinylated anti-rabbit IgG (H + L) vector BA-1000] for assessment of vessel density.

Morphometric Analysis

Alveolarization was assessed by radial alveolar count (RAC) and pulmonary vessel density (PVD) determined using standard methods, as previously reported (29, 45–47). Hearts were dissected and weighed at 14 days of life. The right ventricle (RV) and left ventricle plus septum (LV + S) were

Table 1. *List of antibodies used*

Target	Concentration	Catalog No.	Supplier	RRID
Western blot				
VEGF	1:1,000	sc-7269	Santa Cruz	AB_628430
VEGFR2	1:1,000	55B11	Cell Signaling	AB_2212507
β-actin	1:10,000	A-2228	Sigma	AB_476697
IHC				
vWF	1:1,000	A-0082	Dako	AB_2315604

VEGF, vascular endothelial growth factor; VEGFR2, vascular endothelial growth factor receptor 2; vWF, von Willebrand Factor.

dissected, weighed, and reported as the ratio of RV to LV + S weights.

Lung Function

Lung function was assessed in 14-day-old pups using the flexiVent system (FlexiVent; SCIREQ) to determine total respiratory system resistance and compliance by standard methods, as previously described (28).

Primary Pulmonary Endothelial Cell Isolation

Pulmonary endothelial cells (PECs) were isolated from the lungs of neonatal rat pups (*Day of Life 0*) using standard methods (48). In brief, lungs were isolated, digested with collagenase, filtered serially, and then incubated with anti-CD31-coated magnetic beads (Thermo Scientific). Following incubation, cells were isolated via magnetic separation. PECs were plated on gelatin-coated plates where they were allowed to proliferate in EBM-2 media containing EGM-2 supplements and 10% FBS (Microvascular EBM-2; Lonza). All studies were conducted using first passage (P_1) cells.

In Vitro PEC Growth and Tube Formation Assays

Growth assays were performed using 5,000 PEC cells/well plated on gelatin-coated 48-well plates (Corning). Cells were allowed to adhere at 37°C overnight in EBM-2 media containing EGM-2 supplements. Media were changed every 24 h for up to 5 days, and cells were counted after 5 days of growth. To assess tube formation in PEC, 40,000 cells/well were plated on 24-well plates coated with a rat tail collagen solution. Cells were incubated at 37°C in EBM-2 media containing EGM-2 supplements and 0.5% FBS. After 20 h, 4% paraformaldehyde was added to stop tube formation and fix the PEC before imaging and counting the branch points, as previously described (49). These same studies were conducted with isolated PEC using EGM-2 media supplemented with VEGF (100 ng/mL) (R&D Systems) or 1,25(OH)$_2$D (600 nM) (Cayman Chemical). As described earlier, media were changed daily for 5 days to assess cell proliferation.

Growth assays were conducted using a single-PEC isolation and repeated in triplicate. Tube formation assays were conducted using the same PEC isolation as growth assays, repeated in triplicate with 3–4 images taken/well.

In Vitro PEC Stimulation with 1,25(OH)$_2$D for Quantitative PCR Analysis

At 70%–90% confluence, P_0 PECs were split for P_1 passage before stimulation with 1,25(OH) $_2$D. Once P_1 cells were 70%–90% confluent, cells were incubated overnight in EBM-2 media with 0.5% to optimize the number of cells in G_0/G_1. The next day, media were changed to EBM-2 with 2.5% FBS containing 1,25(OH)$_2$D (600 nM) (Cayman Chemical), and cell pellets were collected following 4 and 24 h of exposure to 1,25(OH)$_2$D.

Whole Lung Western Blot Analysis

Western immunoblots were carried out using standard methods. Briefly, frozen lung samples were homogenized, cellular debris was removed, and protein content was determined by the Bradford method. Samples were resolved by SDS-PAGE, transferred to polyvinylidene difluoride membranes, and then probed with the primary antibodies VEGFR2, VEGF, and β-actin (Table 1). Blots were incubated with the appropriate secondary antibodies conjugated to horseradish peroxidase and visualized by enhanced chemiluminescence (ECL Advance kit; Amersham Pharmacia Biotech). Densitometry was performed using Image Lab (v. 6.1.0 Build 7, Bio-Rad Life Sciences).

PEC RNA Isolation and Analysis

Total RNA was extracted from endothelial cells using the RNEasy kit (Qiagen) per the manufacturer's instructions. Following extraction, total RNA concentration was quantified via BioTek Take 3 microplate (Agilent). Complementary DNA was amplified using the Verso cDNA Synthesis Kit (Thermo Fisher Scientific) following the manufacturer's protocol with 1 μg of total RNA. Real-time quantitative PCR (RT-qPCR) was performed using TaqMan Fast Advanced master mix (Invitrogen) and TaqMan probes (Invitrogen). Probes used for PEC RNA included CYP24A1, VDR, VEGFR2, VEGF, and GAPDH (Table 2). RT-qPCR reactions were cycled on the QuantStudio 7 Flex Real-Time PCR System (Applied Biosystems by Thermo Fisher Scientific). Relative RNA expression was determined using the double-delta cycle threshold (C_t) method (ΔΔCT) using C_t values with a standard deviation below 0.25 between triplicates of each sample and normalized to the endogenous control, GAPDH.

Statistical Approach

Data were assessed for normality using the Shapiro–Wilk test. Normally distributed data are presented as means ± standard error (SE) with statistical analysis conducted using Student's *t* test or one-way analysis of variance (ANOVA) with Sidak's procedure post hoc comparisons. Nonparametric data are presented as median ± interquartile range (IQR) with statistical analysis conducted using the Kruskal–Wallis comparison of mean ranks with Dunn's post hoc comparisons.

Table 2. *List of genes and primers used for quantitative PCR analysis*

Target	Assay ID	Supplier
GAPDH	Rn01775763_g1	TaqMan, Thermo Fisher
Cyp24A1	Rn01423143_m1	TaqMan, Thermo Fisher
VDR	Rn00690616_m1	TaqMan, Thermo Fisher
VEGF	Rn01511602_m1	TaqMan, Thermo Fisher
VEGFR2	Rn00564986_m1	TaqMan, Thermo Fisher

VDR, vitamin D receptor; VEGF, vascular endothelial growth factor; VEGFR2, vascular endothelial growth factor receptor 2.

P values <0.05 were considered significant using a β value of 0.80. Statistical analysis was performed with the Prism software package (v. 10.2.2, GraphPad).

RESULTS

IA 1,25(OH)$_2$D Treatment Improves Distal Lung Alveolar and Vascular Development

At 14 days of life, IA sFlt-1 exposure decreased distal lung airspace development with a 44% [9.0 (SE 0.2) vs. 6.5 (SE 0.2)] reduction in RAC as compared with control pups ($P < 0.05$; Fig. 1, *A* and *B*). Simultaneous treatment of IA sFlt-1-exposed pups with IA 1,25(OH)$_2$D improved distal lung development as demonstrated by a 50% [6.5 (SE 0.2) vs. 9.5 (SE 0.3)] increase in RAC compared with IA sFlt-1 alone ($P < 0.05$; Fig. 1, *A* and *B*). Pups treated with IA 1,25(OH)$_2$D alone did not have statistically significant differences [9.0 (SE 0.2) vs. 9.5 (SE 0.3)] in lung structure compared with control animals (Fig. 1, *A* and *B*).

Paralleling impaired distal airspace development, IA sFlt-1 decreased lung vascular development as demonstrated by a 43% [23.7 (SE 0.6) vs. 13.4 (SE 0.8)] reduction in PVD as compared with control pups ($P < 0.05$; Fig. 2, *A* and *B*). Simultaneous treatment of IA sFlt-1-exposed pups with IA 1,25(OH)$_2$D improved PVD by 56% [13.4 (SE 0.8) vs. 20.9 (SE 0.8)] when compared with pups receiving IA sFlt-1 alone ($P < 0.05$; Fig. 2, *A* and *B*). Associated with an underdeveloped vascular bed, we report that IA sFlt-1 results in RVH. IA sFlt-1 increased right ventricular mass by 48% [0.25 (IQR 0.21–0.27) vs. 0.37 (IQR 0.33–0.39)] compared with controls ($P < 0.05$; Fig. 2*C*). Simultaneous treatment of IA sFlt-1-exposed pups with IA 1,25(OH)$_2$D decreased right ventricular mass by 30% [0.37 (IQR 0.33–0.39) vs. 0.26 (IQR 0.24–0.28)] compared with IA sFlt-1-exposed pups ($P < 0.05$; Fig. 2*C*). Simultaneous treatment of IA sFlt-1-exposed pups with IA 1,25(OH)$_2$D resulted in pulmonary vessel counts [23.7 (SE 0.6) vs. 20.9 (SE 0.8)] and RV mass [0.25 (IQR 0.21–0.27) vs. 0.26 (IQR 0.24–0.28)] measurements no different than control animals (Fig. 2, *A–C*). IA 1,25(OH)$_2$D alone did not change RAC [9.0 (SE 0.2) vs. 9.7 (SE 0.5)], PVD [23.7 (SE 0.6) vs. 22.9 (SE 0.6)], or RV mass [0.25 (IQR 0.21–0.27) vs. 0.25 (IQR 0.24–0.27)] compared with the control group (Fig. 2, *A–C*).

IA 1,25(OH)$_2$D Treatment Improves Lung Function in IA sFlt-1-Exposed Animals

At 14 days of life, pups exposed to IA sFlt-1 demonstrated increased total respiratory system resistance by 42% [0.53 (IQR 0.5–0.56) vs. 0.74 (IQR 0.63–0.92)] and decreased total respiratory compliance by 30% [0.039 (IQR 0.037–0.045) vs. 0.027 (IQR 0.019–0.034)] as compared with control pups ($P < 0.05$; Fig. 3, *A* and *B*). Simultaneous treatment of IA sFlt-1-exposed pups with IA 1,25(OH)$_2$D decreased total respiratory resistance by 37% [0.74 (IQR 0.63–0.92) vs. 0.52 (IQR 0.38–0.58)] and increased compliance by 36% [0.027 (IQR 0.019–0.034) vs. 0.032 (IQR 0.029–0.05)] compared with pups exposed to IA sFlt-1 alone ($P < 0.05$; Fig. 3, *A* and *B*), resulting in restoration of resistance [0.53 (IQR 0.5–0.56) vs. 0.52 (IQR 0.38–0.58)] and compliance [0.039 (IQR 0.037–0.045) vs. 0.032 (IQR 0.029–0.05)] similar to that of control animals (Fig. 3, *A* and *B*). Animals exposed to IA 1,25(OH)$_2$D alone did not demonstrate changes in total respiratory system resistance [0.53 (IQR 0.5–0.56) vs. 0.47 (IQR 0.45–0.53)] or compliance [0.039 (IQR 0.037–0.045) vs. 0.041 (IQR 0.038–0.045)] compared with control animals (Fig. 3, *A* and *B*). There were no differences detected in study endpoints (distal lung structure, RVH, lung function) between males and females across all study groups.

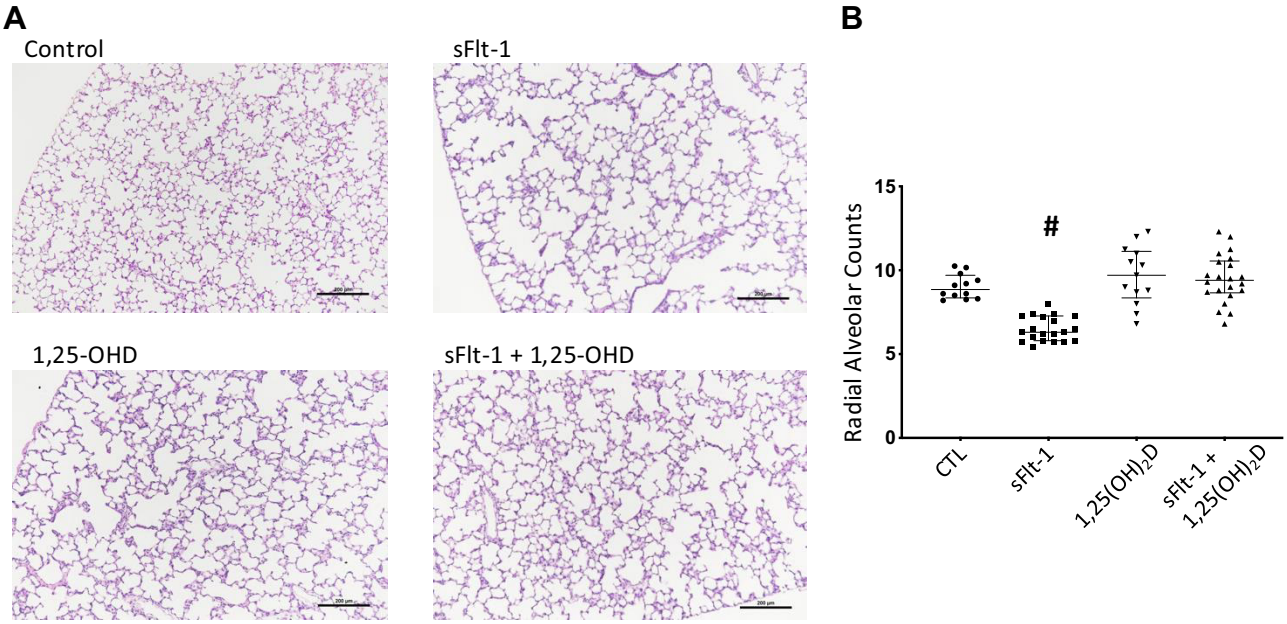

Figure 1. Effects of IA 1,25(OH)$_2$D treatment on lung structure on IA sFlt-1-induced experimental BPD. *A*: representative micrographs were obtained at the same magnification (scale bars, 200 μm). *B*: in comparison with IA sFlt-1 exposure, IA 1,25(OH)$_2$D treatment improved septation and decreased lung simplification as quantified by radial alveolar counts (RAC). Statistical analysis was conducted via ANOVA with Sidak's post hoc procedure. #$P < 0.05$ compared with all groups. Data are represented as means ± SE, with individual data points representing individual animals. $n = 11–23$ animals/group. 1,25(OH)$_2$D, 1,25 dihydroxyvitamin D; BPD, bronchopulmonary dysplasia; CTL, control animals; IA, intraamniotic; sFlt-1, soluble fms-like tyrosine kinase 1.

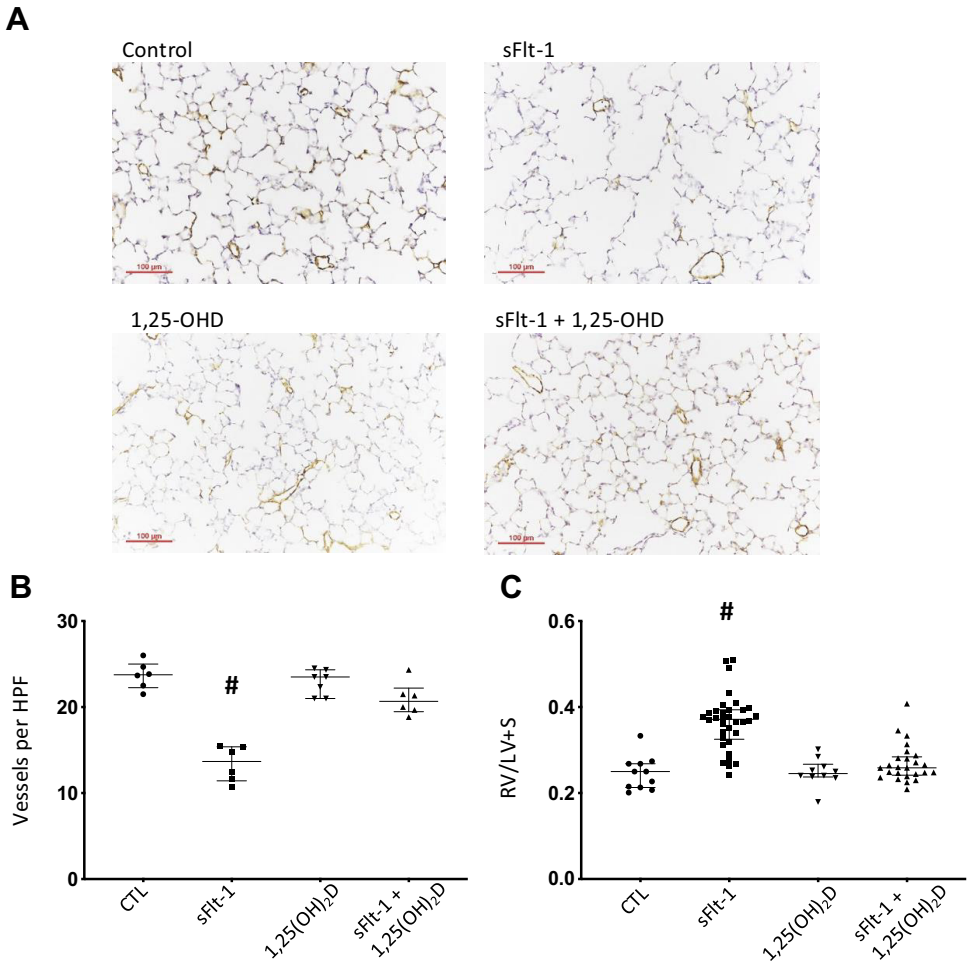

Figure 2. Effects of IA $1,25(OH)_2D$ treatment on pulmonary vessel development and right ventricle mass in IA sFlt-1-induced experimental BPD. *A*: representative images of endothelial immunostaining with von Willebrand factor were obtained at the same magnification (scale bars, 100 μm). *B*: IA $1,25(OH)_2D$ treatment of IA sFlt-1-exposed pups increased pulmonary vessel density when compared with pups exposed to IA sFlt-1 alone. Compared with control pups, pulmonary vessel density was similar following IA $1,25(OH)_2D$ treatment of IA sFlt-1-exposed pups as assessed at 14 days. *C*: right ventricular hypertrophy (RVH) induced by IA sFlt-1 injection was prevented with IA $1,25(OH)_2D$ treatment. RV/LV + S data represented as median with interquartile range and vessels per HPF represented as means ± SE. Individual data points represent individual animals. $n = 11–23$ animals/group for RVH measurements, 6 animals/group for vessel density. Statistical analysis was conducted via ANOVA with Sidak's post hoc procedure for vessel density and Kruskal–Wallis comparison of mean ranks with Dunn's post hoc comparisons. $\#P < 0.05$ compared with all groups. $1,25(OH)_2D$, 1,25 dihydroxyvitamin D; BPD, bronchopulmonary dysplasia; CTL, control animals; HPF, high powered field (×40); IA, intraamniotic; LV + S, left ventricle plus septum; RV, right ventricle; sFlt-1, soluble fms-like tyrosine kinase 1.

Neonatal Pulmonary Endothelial Cell Growth and Tube Formation Are Impaired Following IA sFlt-1 Exposure In Vitro

We found that isolated primary PEC from newborn pups exposed to IA sFlt-1 had decreased growth and tube formation by 55% [50,250 (SE 750) vs. 22,750 (SE 660)] and 26% [101 (SE 5.4) vs. 75 (SE 3.3)], respectively, as compared with PEC isolated from control newborn pups ($P < 0.05$; Fig. 4, *A–C*). PEC isolated from newborn pups simultaneously treated with IA $1,25(OH)_2D$ during IA sFlt-1 exposure demonstrated increased PEC growth by 63% [22,750 (SE 660) vs. 37,000 (SE 1521)] compared with PEC from animals exposed to IA sFlt-1 alone ($P < 0.05$), but absolute growth

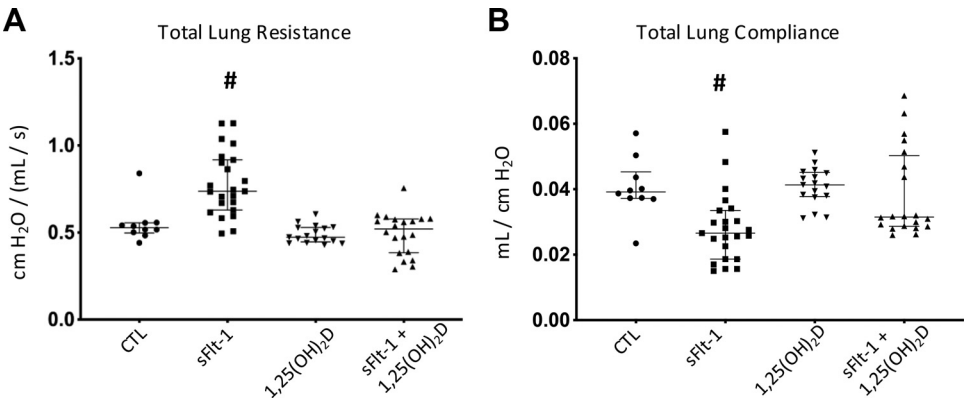

Figure 3. Effects of IA $1,25(OH)_2D$ treatment on lung resistance (*A*) and compliance (*B*) in IA sFlt-1-induced experimental BPD. IA $1,25(OH)_2D$ treatment improved lung mechanics at *day 14* in comparison with pups who received IA sFlt-1 only. Compared with control pups, lung mechanics were similar following IA $1,25(OH)_2D$ treatment of IA sFlt-1-exposed pups. Data represented as median with interquartile range with individual data points representing individual animals, $n = 10–23$ animals/group. Statistical analysis was conducted via Kruskal–Wallis comparison of mean ranks with Dunn's post hoc comparison. $\#P < 0.05$ compared with all groups. $1,25(OH)_2D$, 1,25 dihydroxyvitamin D; BPD, bronchopulmonary dysplasia; CTL, control animals; IA, intraamniotic; sFlt-1, soluble fms-like tyrosine kinase 1.

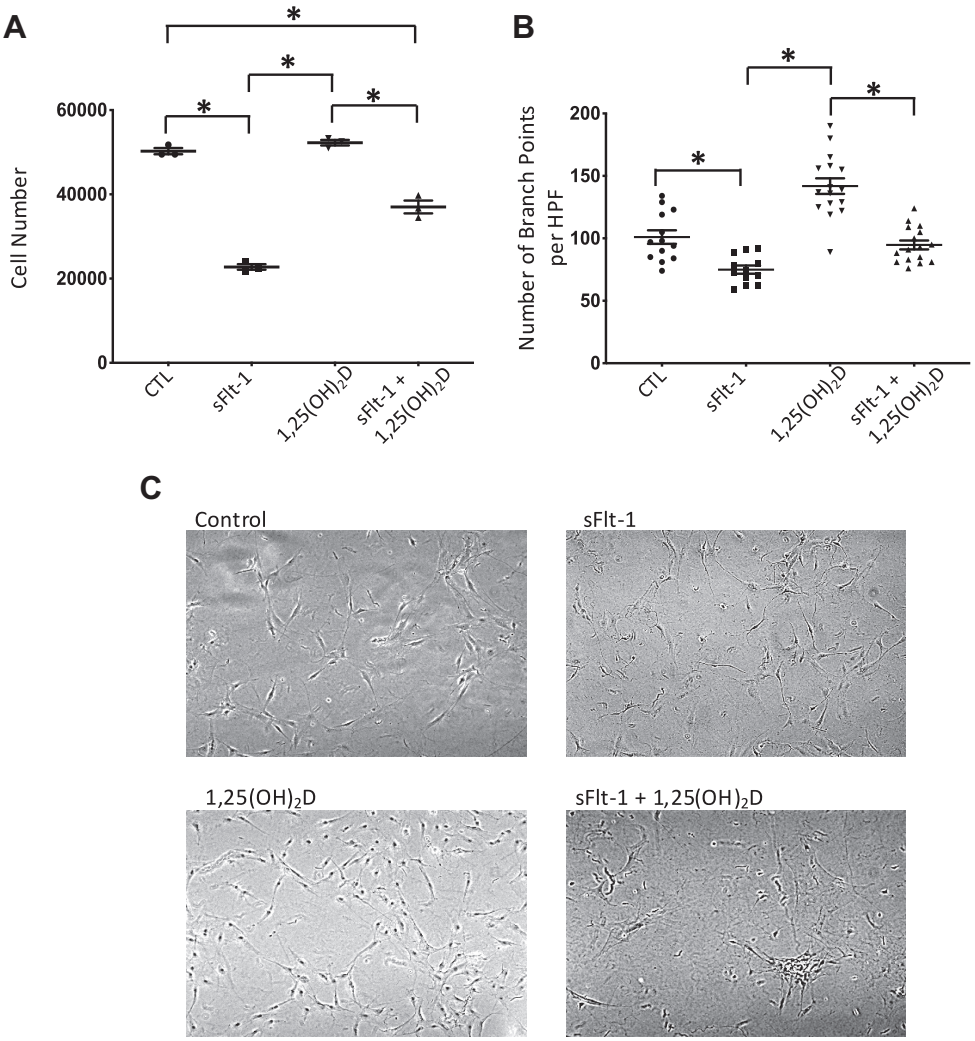

Figure 4. IA $1,25(OH)_2D$ treatment of IA sFlt-1-exposed pups improved in vitro neonatal PEC growth and tube formation. *A*: absolute PEC growth assessed after 5 days was decreased following IA sFlt-1. IA $1,25(OH)_2D$ improved but did not fully restore PEC growth. *B*: PEC tube formation was impaired following IA sFlt-1 exposure and restored with IA $1,25(OH)_2D$ treatment. Exposure to IA $1,25(OH)_2D$ alone increased tube formation. *C*: representative images of PEC tube formation in 2.5% FBS EGM-2 media. Data represented as means ± standard error. Growth assay data are presented as 3 technical replicates/group, and tube formation is presented with each data point representing the quantification of an individual HPF combined from 3 to 4 technical replicates/group. Both growth and tube formation assays were conducted using the same PEC isolation at P_1. Statistical analysis was conducted via ANOVA with Sidak's post hoc procedure. *$P < 0.05$. $1,25(OH)_2D$, 1,25 dihydroxyvitamin D; BPD, bronchopulmonary dysplasia; CTL, control animals; HPF, high powered field (×40); IA, intra-amniotic; PEC, pulmonary endothelial cell; sFlt-1, soluble fms-like tyrosine kinase 1.

remained 26% [50,250 (SE 750) vs. 37,000 (SE 1521)] below control PEC growth ($P < 0.05$; Fig. 4*A*). PEC isolated from animals treated with IA $1,25(OH)_2D$ alone did not demonstrate significant changes in PEC growth from that of control animals [50,250 (SE 750) vs. 52,250 (SE 660)] (Fig. 4*A*).

PEC isolated from pups simultaneously exposed to IA sFlt-1 and IA $1,25(OH)_2D$ demonstrated increased tube formation by 26% [75 (SE 3.3) vs. 95 (SE 3.6)] compared with PEC from animals exposed to IA sFlt-1 alone ($P < 0.05$; Fig. 4, *B* and *C*). PEC isolated from pups exposed to simultaneous IA sFlt-1 and IA $1,25(OH)_2D$ demonstrated tube formation no different [101 (SE 5.4) vs. 95 (SE 3.6)] than PEC from control pups ($P > 0.05$; Fig. 4, *B* and *C*). PEC isolated from newborn pups exposed to IA $1,25(OH)_2D$ alone had increased tube formation by 40% [101 (SE 5.4) vs. 142 (SE 6.3)] compared with PEC isolated from control newborn pups ($P < 0.05$; Fig. 4, *B* and *C*).

Isolated Neonatal Pulmonary Endothelial Cells Retain the Ability to Respond to VEGF In Vitro

To understand the impact of IA exposures on the ability of PEC to respond to VEGF, we assessed PEC growth and tube formation following the addition of VEGF to standard EGM-2 media using cells isolated from all IA exposure groups. PEC isolated from control animals treated with VEGF demonstrated increased growth by 30% [50,250 (SE 750) vs. 66,750 (SE 1300)] and tube formation by 34% [101 (SE 5.4) vs. 135 (SE 3.9)] ($P < 0.05$; Figs. 5 and 6). PEC from IA sFlt-1 alone pups treated with VEGF demonstrated increased growth by 43% [22,750 (SE 661) vs. 32,500 (SE 1,100)] compared with PEC from IA sFlt-1 pups under standard EGM2 media conditions ($P < 0.05$; Fig. 5). VEGF stimulation of PEC isolated from IA sFlt-1 pups increased tube formation by 42% [75 (SE 3.3) vs. 107 (SE 4.3)] compared with standard EGM2 media conditions ($P < 0.05$; Fig. 6). PEC isolated from pups simultaneously exposed to IA sFlt-1 and IA $1,25(OH)_2D$ demonstrated increased growth by 24% [3,700 (SE 1,520) vs. 45,500 (SE 900)] when stimulated with VEGF compared with growth under standard EGM2 media conditions ($P < 0.05$; Fig. 5). VEGF-stimulated PEC isolated from pups simultaneously exposed to IA sFlt-1 and IA 1,25-OHD increased tube formation by 48% [95 (SE 3.6) vs. 141 (SE 6.3)] compared with standard EGM2 media conditions ($P < 0.05$; Fig. 6). PEC isolated from pups treated with IA $1,25(OH)_2D$ alone demonstrated increased growth by 53% [52,250 (SE 660) vs. 79,500 (SE 2500)] and tube formation by 21% [142 (SE 6.3) vs. 172 (SE 5.9)] compared with standard EGM2 media conditions when stimulated with VEGF ($P < 0.05$; Figs. 5 and 6).

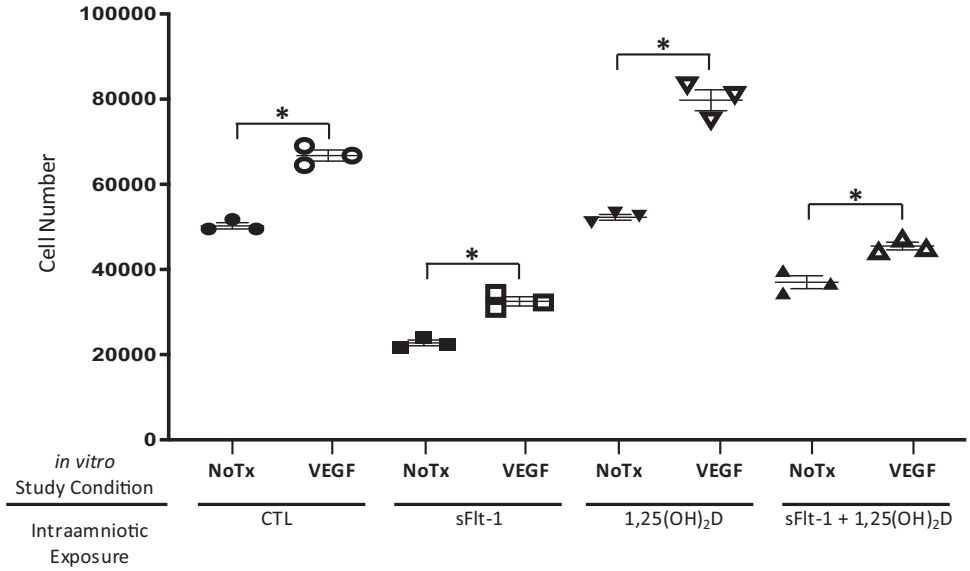

Figure 5. In vitro stimulation with VEGF increases neonatal PEC growth. PEC isolated from IA sFlt-1-exposed pups maintained the ability to increase growth in response to VEGF. IA $1,25(OH)_2D$ treatment of IA sFlt-1-exposed pups led to increased absolute PEC growth following in vitro VEGF stimulation compared with standard EGM. Data represented as means ± standard error. Growth assay data are presented as 3 technical replicates/group using the same PEC isolation at P_1. Statistical analysis was conducted via ANOVA with Sidak's post hoc procedure. $^*P < 0.05$. CTL, control animals; NoTx, no additional treatment, standard EGM only; PEC, pulmonary endothelial cell; sFlt-1, soluble fms-like tyrosine kinase 1; VEGF, vascular endothelial growth factor.

In Vitro Stimulation of Neonatal Pulmonary Endothelial Cells with $1,25(OH)_2D$ Increases Growth and Tube Formation

To understand if $1,25(OH)_2D$ has a direct impact on PEC growth and tube formation, we treated isolated primary PECs, from all intraamniotic exposure groups, with $1,25(OH)_2D$ in standard EGM-2 media. PEC isolated from control animals treated with in vitro $1,25(OH)_2D$ demonstrated increased growth by 22% [50,250 (SE 750) vs. (60,250 (SE 1300)] and tube formation by 25% [101 (SE 5.4) vs. 126 (5.3)] compared with standard EGM2 media conditions ($P < 0.05$; Figs. 7 and 8). PEC isolated from pups exposed to IA sFlt-1 alone treated with in vitro $1,25(OH)_2D$ demonstrated increased growth by 49% [22,750 (SE 660) vs. 34,000 (SE 500)] compared with PEC isolated from pups exposed to IA sFlt-1 alone under standard EGM2 media conditions ($P < 0.05$; Fig. 7); however, there was not a significant increase [75 (SE 3.3) vs. 81 (SE 4.6)] in tube formation compared with standard EGM2 media conditions (Fig. 8). PEC isolated from pups simultaneously exposed to IA sFlt-1 and IA $1,25(OH)_2D$ demonstrated increased growth by 22% [37,000 (SE 1500) vs. 42,750 (SE 1100)] when stimulated with in vitro $1,25(OH)_2D$ compared with growth under standard EGM2 media conditions ($P < 0.05$; Fig. 7). In vitro $1,25(OH)_2D$ stimulation of PEC isolated from pups simultaneously exposed to IA sFlt-1 and IA $1,25(OH)_2D$ increased tube formation by 23% [95 (SE 3.6) vs. 117 (SE 5.5)] compared with standard EGM2 media conditions ($P < 0.05$; Fig. 8). PEC isolated from pups treated with IA $1,25(OH)_2D$ alone demonstrated increased growth by 57% [52,250 (SE 660) vs. 82,000 (SE 660)] ($P < 0.05$; Fig. 7), but tube formation was not significantly different [142 (SE 6.3) vs. 158 (SE 6.1)] compared with standard EGM2 media conditions when stimulated with $1,25(OH)_2D$ (Fig. 8).

IA $1,25(OH)_2D$ Treatment Increases VEGFR2 and VEGF in the Neonatal Lung

To explore the mechanisms of IA $1,25(OH)_2D$ treatment-induced improvements in lung development, we assessed protein levels of VEGF and the key VEGF signal transducer,

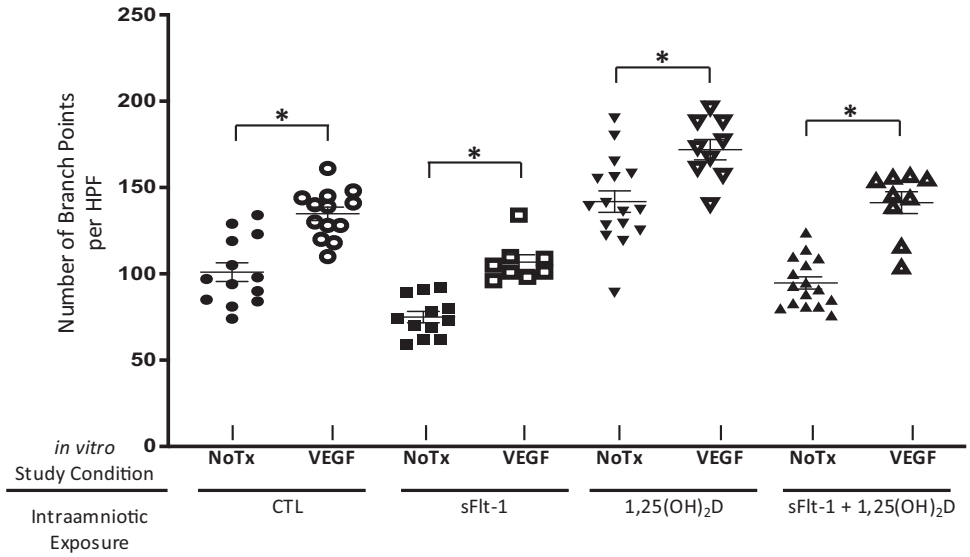

Figure 6. In vitro stimulation with VEGF increases neonatal PEC tube formation. PEC isolated from IA sFlt-1-exposed pups maintained the ability to increase tube formation in response to VEGF. IA $1,25(OH)_2D$ treatment of IA sFlt-1-exposed pups led to increased branching following in vitro VEGF stimulation compared with standard EGM. Tube formation data are presented with each data point representing the quantification of an individual HPF combined from 3 to 4 technical replicates/group using the same PEC isolation at P_1. Statistical analysis was conducted via ANOVA with Sidak's post hoc procedure. $^*P < 0.05$. $1,25(OH)_2D$, 1,25 dihydroxyvitamin D; CTL, control animals; HPF, high powered field (×40); IA, intraamniotic; NoTx, no additional treatment, standard EGM only; PEC, pulmonary endothelial cell; sFlt-1, soluble fms-like tyrosine kinase 1; VEGF, vascular endothelial growth factor.

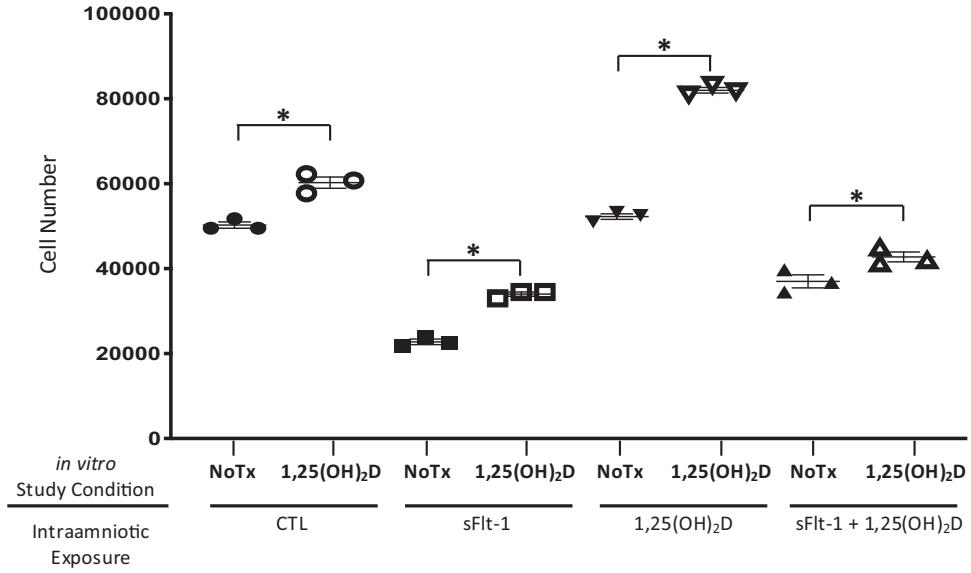

Figure 7. In vitro stimulation with IA $1,25(OH)_2D$ increases neonatal PEC growth. IA $1,25(OH)_2D$ stimulation of PEC from control animals increased growth compared with standard EGM while also increasing PEC growth following IA sFlt-1. IA $1,25(OH)_2D$ treatment of IA sFlt-1-exposed pups led to increased growth following in vitro $1,25(OH)_2D$ stimulation compared with standard EGM. Data represented as means ± standard error. Growth assay data are presented as 3 technical replicates/group using the same PEC isolation at P_1. Statistical analysis was conducted via ANOVA with Sidak's post hoc procedure. *$P <$ 0.05. $1,25(OH)_2D$, 1,25 dihydroxyvitamin D; CTL, control animals; IA, intraamniotic; NoTx, no additional treatment, standard EGM only; PEC, pulmonary endothelial cell; sFlt-1, soluble fms-like tyrosine kinase 1.

VEGFR2, in neonatal lungs. IA sFlt-1-exposed pups did not demonstrate a significant difference in whole lung VEGFR2 [0.49 (SE 0.11) vs. 0.53 (SE 0.06)] or VEGF [0.44 (SE 0.05) vs. 0.39 (SE 0.03)] content as compared with controls (Fig. 9). Pups treated with IA $1,25(OH)_2D$ alone did not demonstrate significant changes in whole lung content of VEGFR2 [0.49 (SE 0.11) vs. 0.71 (SE 0.06)] or VEGF [0.44 (SE 0.05) vs. 0.67 (SE 0.02)] compared with control animals (Fig. 9). Simultaneous treatment with IA 1,25 $(OH)_2D$ during IA sFlt-1 exposure increased whole lung content of VEGFR2 by 100% [0.53 (SE 0.06) vs. 1.08 (SE 0.11)] ($P < 0.05$; Fig. 9*A*) and increased VEGF content by 68% [0.39 (SE 0.03) vs. 0.75 (SE 0.12)] compared with IA sFlt-1 alone ($P < 0.05$; Fig. 9*B*). Simultaneous treatment with IA $1,25(OH)_2D$ during IA sFlt-1 exposure increased whole lung content of VEGFR2 by 120% [0.49 (SE 0.11) vs. 1.08 (SE 0.11)] ($P < 0.05$; Fig. 9*A*) and increased VEGF content by 45% [0.44 (SE 0.05) vs. 0.75 (SE 0.12)] compared with control animals ($P < 0.05$; Fig. 9*B*).

In Vitro $1,25(OH)_2D$ Increases VEGFR2 Expression in Neonatal Pulmonary Endothelial Cells

To delineate possible mechanisms by which $1,25(OH)_2D$ increases PEC growth and tube formation, we assessed in vitro changes in key vitamin D regulatory genes, VDR and CYP24A1, and both VEGF and VEGFR2 following $1,25(OH)_2D$ stimulation of PEC isolated from control pups. Following 24 h of stimulation with $1,25(OH)_2D$, VDR expression increased 100% [1.09 (SE 0.21) vs. 2.23 (SE 0.41)] compared with expression at 4 h of stimulation ($P < 0.05$; Fig. 10*A*). CYP24A1 expression increased 32-fold [1.47 (SE 0.84) vs. 32.77 (SE 7.77)] compared with expression after 4 h of $1,25(OH)_2D$ exposure ($P < 0.05$; Fig. 10*B*). After 24 h of stimulation with $1,25(OH)_2D$, VEGFR2 expression increased sixfold [1.05 (SE 0.17) vs. 6 (SE 1.73)] compared with expression at 4 h of stimulation ($P < 0.05$; Fig. 10*C*). After 24 h of stimulation with $1,25(OH)_2D$, VEGF expression decreased 50% [1.04 (SE

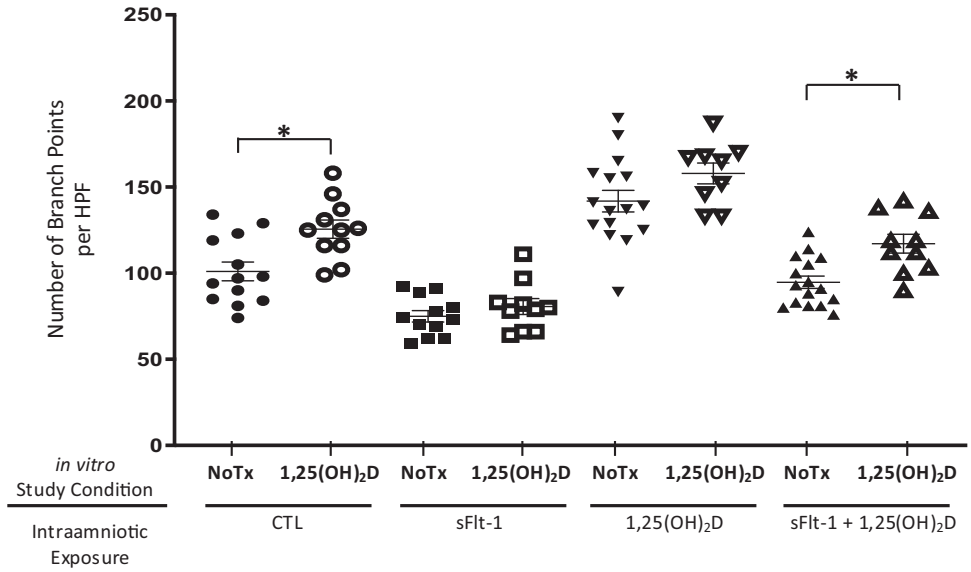

Figure 8. In vitro stimulation with $1,25(OH)_2D$ increases neonatal PEC tube formation. $1,25(OH)_2D$ increased tube formation in control PEC but did not increase tube formation in PEC isolated from IA sFlt-1-exposed pups. IA $1,25(OH)_2D$ treatment of IA sFlt-1-exposed pups led to increased branching following in vitro $1,25(OH)_2D$ stimulation compared with standard EGM. Tube formation data are presented with each data point representing the quantification of an individual HPF combined from 3 to 4 technical replicates/group using the same PEC isolation at P_1. Statistical analysis was conducted via ANOVA with Sidak's post hoc procedure. *$P <$ 0.05. $1,25(OH)_2D$, 1,25 dihydroxyvitamin D; CTL, control animals; HPF, high powered field (×40); IA, intraamniotic; NoTx, no additional treatment, standard EGM only; PEC, pulmonary endothelial cell; sFlt-1, soluble fms-like tyrosine kinase 1.

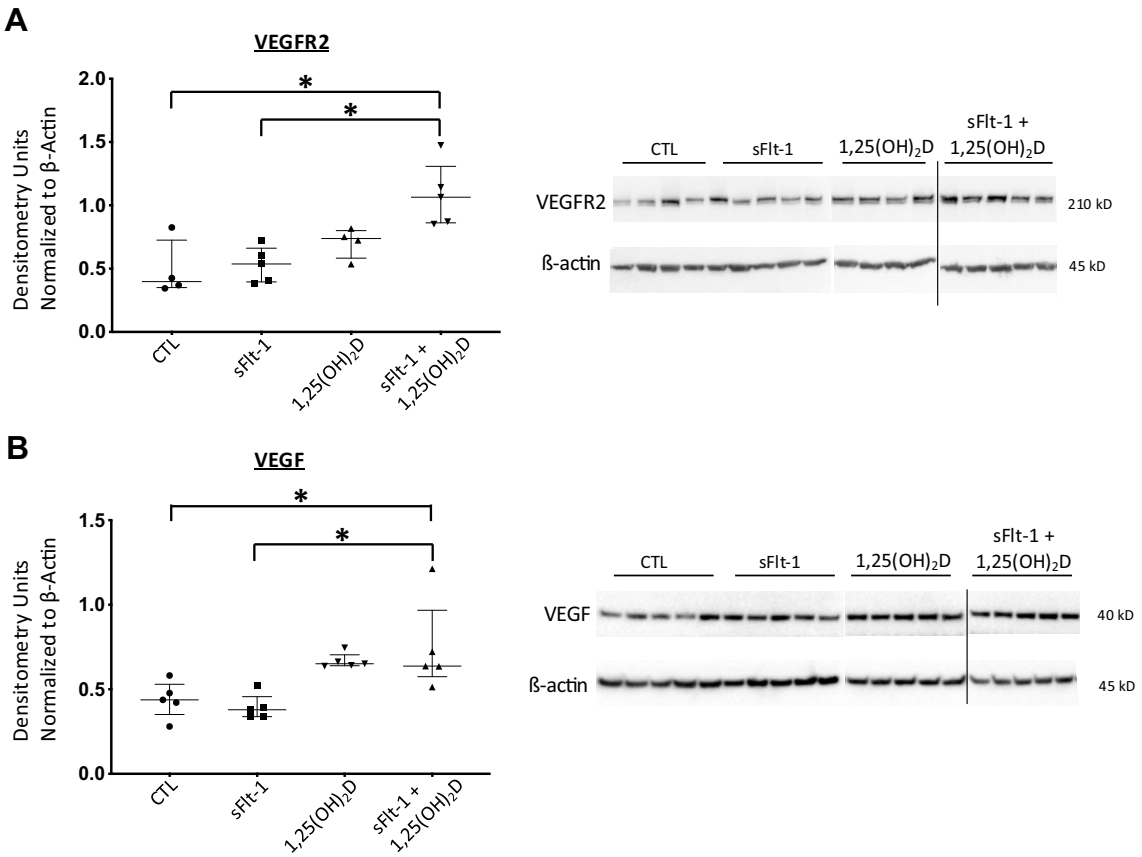

Figure 9. Effect of IA 1,25(OH)$_2$D treatment on VEGFR2 and VEGF expression in the newborn lung at birth. *A*: simultaneous IA 1,25(OH)$_2$D treatment of IA sFlt-1-exposed pups increases VEGFR2 content at birth in IA sFlt-1-induced experimental BPD. VEGFR2 content was not different in the IA sFlt-1 group compared with controls. *B*: simultaneous IA 1,25(OH)$_2$D treatment of IA sFlt-1-exposed pups increases VEGF content at birth. VEGFR2 content was not different in the IA sFlt-1 group compared with controls. $^*P < 0.05$. Data are represented as means ± SE, with individual data points representing individual animals. $n = 4$ or 5/group. Statistical analysis was conducted via ANOVA with Sidak's post hoc procedure. The vertical line denotes contiguous samples, run on the same gel, that were reordered to align with the histogram presentation. 1,25(OH)$_2$D, 1,25 dihydroxyvitamin D; BPD, bronchopulmonary dysplasia; CTL, control animals; IA, intraamniotic; sFlt-1, soluble fms-like tyrosine kinase 1; VEGFR2, vascular endothelial growth factor receptor 2.

0.17) vs. 0.49 (SE 0.09)] compared with expression at 4 h of stimulation ($P < 0.05$; Fig. 10*D*).

DISCUSSION

In the current study, we report that IA sFlt-1, used to mimic the intrauterine environment of preeclampsia, caused sustained abnormalities of lung growth, decreased lung function, and RVH in infant rats. These structural and functional changes were associated with early postnatal impairments in PEC growth and tube formation in vitro. We demonstrate that simultaneous administration of IA 1,25(OH)$_2$D with IA sFlt-1 exposure of fetal pups preserves distal lung structure, pulmonary vascular development, and pulmonary function while preventing RVH in infant rats. Our in vitro findings demonstrate that primary PEC isolated from IA sFlt-1-exposed newborn rat lungs show decreased in vitro growth and tube formation compared with PEC isolated from control newborn pups. We also found PEC isolated from newborn pups treated with IA 1,25(OH)$_2$D during IA s-Flt exposure demonstrated improved in vitro growth and tube formation.

The current study is, to our knowledge, the first to demonstrate the therapeutic potential of 1,25(OH)$_2$D to improve distal lung and vascular development during IA sFlt-1 exposure in an animal model of BPD. Interestingly, treatment with IA 1,25(OH)$_2$D mitigates the decrease in PEC growth and tube formation observed following IA sFlt-1 exposure. Our studies extended beyond the in vivo effects of IA 1,25(OH)$_2$D by describing the exciting effect of 1,25(OH)$_2$D to increase neonatal PEC growth not only in isolated PECs from control animals but also those exposed to IA sFlt-1. Finally, these data demonstrate that 1,25(OH)$_2$D increases VEGFR2 expression in both the whole lung and in isolated PECs. Overall, our data suggest that 1,25(OH)$_2$D has proangiogenic effects in the developing lung exposed to IA sFlt-1 and that these effects are mediated through direct improvements in PEC growth and tube formation capacity.

Past experimental work has demonstrated that pulmonary angiogenesis is necessary for appropriate alveolar development (13, 14). VEGF inhibition at birth interrupts critical pulmonary angiogenesis and leads to alveolar simplification in infant rats (14, 50). These animal studies, combined with clinical data indicating that infants dying from BPD had decreased concentrations of lung proangiogenic factors, led to the development of the "vascular hypothesis of BPD" in which impaired angiogenesis leads to the decreased distal lung development characteristic of BPD (12, 15). Specifically, endothelial-epithelial cell cross talk through angiocrine

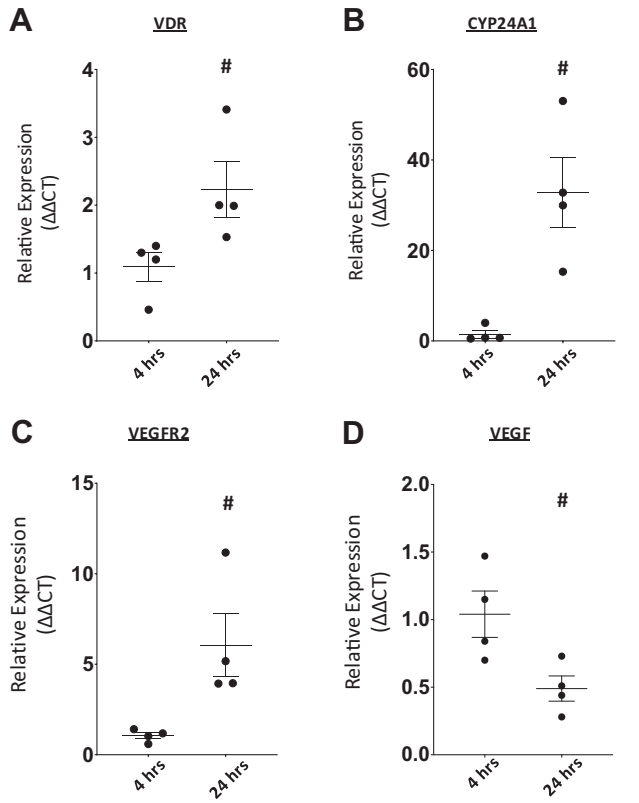

Figure 10. PEC isolated from healthy neonatal lungs increases VEGFR2 expression following stimulation with 1,25(OH)$_2$D. *A* and *B*: PEC appropriately responds to exogenous 1,25(OH)$_2$D by increasing vitamin D receptor (VDR) and the primary vitamin D catabolism enzyme, CYP24A1. *C*: VEGFR2 expression increases following in vitro 1,25(OH)$_2$D stimulation. *D*: VEGF expression decreases following in vitro 1,25(OH)$_2$D stimulation. Data represented as means ± standard error, with each data point representing an individual PEC isolation. Statistical analysis was conducted via unpaired Student's *t* test. #$P < 0.05$. 1,25(OH)$_2$D, 1,25 dihydroxyvitamin D; IA, intraamniotic; PEC, pulmonary endothelial cell; VEGFR2, vascular endothelial growth factor receptor 2.

signaling is critical to the coordination of the developing distal lung epithelium alongside the pulmonary vasculature. In addition to VEGF, other paracrine factors including nitric oxide, insulin-like growth factor-1, retinoic acid, and hepatocyte growth factor are likely to be involved in the complementary development of the lung endothelium and epithelium (51–53). Recent work has highlighted that VEGF expressed from alveolar type 1 epithelial cells in the mouse lung is required for proper alveolarization and maintenance of the alveolar subtype of endothelial cells (54).

Beyond alveolarization, optimizing endothelial function and vascular growth in the perinatal period may reduce the morbidity and mortality associated with BPD and BPD-associated PH (BPD-PH). Infants with early PH detected by echocardiography in the first week of life were at greater risk for the development of late PH and worse BPD than those without early PH (55). Compounding the early vascular disease associated with BPD, exposure of the developing endothelium to stressors such as hypoxia, hyperoxia, and inflammation may lead to endothelial cell injury that further disrupts development in the postnatal period, increasing the risk of pulmonary vascular disease later in life (56).

In the current study, we show the importance of PEC in the pathogenesis of experimental BPD associated with the inhibition of VEGF signaling with IA sFlt-1. Our data demonstrate that PEC isolated at birth from animals exposed to IA sFlt-1 have decreased in vitro growth and tube formation, likely secondary to a loss in VEGF paracrine signaling leading to disrupted alveolarization, independent of postnatal insults, which may further impair PEC growth and function. Our laboratory has previously shown that IA sFlt-1 results in disrupted VEGF signaling in the neonatal lung and that restoration of perinatal VEGF signaling with a monoclonal antibody to sFlt-1, following IA sFlt-1 exposure, prevented experimental BPD (28, 29). Our findings add to these prior studies by demonstrating that in vitro stimulation of PEC from animals exposed to IA sFlt-1 with VEGF improved but did not fully rescue the phenotype, suggesting that while PEC health can be improved postnatally there may exist limitations to postnatal interventions. Emerging research from human lung samples and in rodent models has both defined subpopulations of lung endothelial cells and described differential responses to injury across the developmental timeline (57–59). Future work addressing both initial drivers of PEC phenotypic change and response to postnatal stress following IA sFlt-1 will better inform our understanding of phenotypic diversity in experimental BPD. Given the central role of endothelial cells in the pathogenesis of BPD and BPD-PH, therapies that enhance perinatal endothelial cell health will likely improve postnatal lung development and reduce the burden of BPD.

We have previously demonstrated that 1,25(OH)$_2$D administered via IA injection improved lung development, prevented pulmonary hypertension, and improved placental vascular development in a rat model of chorioamnionitis (42, 43). Before these studies, vitamin D research had largely focused on the anti-inflammatory properties of 1,25(OH)$_2$D. However, we demonstrated the proangiogenic effect of 1,25(OH)$_2$D to increase pulmonary artery endothelial cell growth and increase expression of VEGFR2 and VEGF in the neonatal lung (42). Our current study further supports the proangiogenic properties of 1,25(OH)$_2$D by demonstrating that 1,25(OH)$_2$D improves early postnatal PEC growth both when simultaneously administered with sFlt-1 antenatally and when administered in vitro to PECs isolated from pups exposed to IA sFlt-1. The positive effect of 1,25(OH)$_2$D demonstrated in the current study is likely related to enhanced endothelial health through the restoration of the endothelial-epithelial VEGF signaling axis during the late canalicular stage of lung development.

Alignment of the pulmonary vasculature and developing airspace is dependent on angiocrine cross talk between epithelial and endothelial cells in the developing lung. Specifically, VEGF secreted from lung epithelial cells provides both a survival signal and direction to underlying endothelial cells that in turn support epithelial cell-mediated septation (53, 54). As such, a proposed mechanism for sFlt-1-induced lung injury and the therapeutic effect of 1,25(OH)$_2$D is as follows. Antenatally, sFlt-1 binds VEGF in the developing lung, limits local concentrations of VEGF, and decreases VEGF binding to PECs. Loss of VEGF signal results in aberrant PEC function, subsequent loss of reciprocal angiocrine signaling, and the resultant decrease in distal lung and vascular

development. Consistent with prior studies, our data support that treatment with 1,25$(OH)_2$D increases both VEGF and VEGFR2 content in the neonatal lung, preserving critical PEC signaling (41). Although the present study indicates that direct stimulation of isolated PEC with 1,25$(OH)_2$D decreases VEGF expression, we hypothesize that the increase in whole lung VEGF content is mediated through increased pulmonary epithelial cell expression. Lung alveolar epithelial cells are known to express VDR and produce essential VEGF needed for alveolarization (35, 39, 54). Future studies focused on the different types of resident lung cells, including epithelial cells, are needed to inform our understanding of how 1,25$(OH)_2$D improves early lung development through potentially different and cell-specific mechanisms.

Treatment with 1,25$(OH)_2$D increases PEC expression of VEGFR2, the primary mediator of VEGF signaling in endothelial cells. The increase in VEGFR2 increases PEC function, resulting in improved angiocrine signaling. Sustaining endothelial health in this critical window preserves vascular development, prevents pulmonary hypertension, and optimizes alveolar growth. The postnatal period for infants born prematurely places them at risk for additional lung injury, including hyperoxia and mechanical ventilation. Whether IA sFlt-1 exposure increases susceptibility to postnatal injuries remains an important question for future study. In addition, angiogenesis and alveolarization continue postnatally, and whether the early changes in postnatal PEC growth and function persist throughout development are unknown and require future study.

This study has potential limitations. Since we use a single sFlt-1 injection directly into the amniotic cavity during late gestation, this model does not fully recapitulate the complex intrauterine environment associated with preeclampsia pathogenesis nor does it account for the prolonged exposure to antiangiogenic peptides that a human fetus may be exposed to. Although this is a limitation, we highlight that an excess of a single antiangiogenic peptide, sFlt-1, is sufficient to mimic lung histology similar to BPD. We have previously reported that growth restriction is not evident in this model, which is a common complication of neonates born to mothers with preeclampsia (29). However, the development of experimental BPD without growth restriction informs the importance of how early derangements in pulmonary angiogenesis are sufficient to impair lung development without growth restriction. In addition, pulmonary endothelial cells within the developing lung arise from various subpopulations of arterial, venous, lymphatic, or capillary origin (57, 58, 60). Although isolation of primary PECs is a powerful and essential tool to understand endothelial cell biology, isolation of PECs from the whole lung makes inferences about subpopulations and cell-cell interactions difficult. Future studies are needed to understand the contribution of these different pulmonary endothelial cell subtypes and the impact of 1,25$(OH)_2$D on endothelial cell biology. Finally, 1,25$(OH)_2$D treatment was provided directly into the amniotic space. This route provides important information on the impact of 1,25$(OH)_2$D in the developing endothelium but limits the translational nature of therapy. Our study does suggest that maternal supplementation with vitamin D could be a therapeutic option to improve neonatal pulmonary development in the setting of elevated intraamniotic sFlt-1 concentrations as seen in preeclampsia. Specifically, the current study utilized the active hormone 1,25$(OH)_2$D which would ultimately be the metabolite fetuses are exposed to after placental metabolism of 25-hydroxyvitamin D [25$(OH)_2$D] to 1,25$(OH)_2$D (61, 62). Future studies examining the therapeutic role of 1,25$(OH)_2$D by maternal or postnatal routes are indicated to further assess the role of vitamin D as a therapy to reduce the burden of BPD. Multiple rodent studies have demonstrated a therapeutic effect of 1,25$(OH)_2$D when used in postnatal exposure models of BPD (63–66).

In summary, we report that IA 1,25$(OH)_2$D treatment preserves distal alveolar and pulmonary vascular growth, restores normal lung function, and prevents RVH in pups exposed to IA sFlt-1 during the late canalicular stage of rat lung development. We demonstrate that the positive in vivo treatment effects of 1,25$(OH)_2$D are associated with in vitro improvements in growth and tube formation utilizing primary PEC isolated from our model. We conclude that 1,25$(OH)_2$D has proangiogenic effects that are protective for the fetal rat lung in experimental BPD due to IA sFlt-1. We speculate that sFlt-1-induced disruption of VEGF-mediated endothelial-epithelial cell cross talk in the developing lung contributes to preeclampsia-related BPD. Future insights into the mechanisms underlying the development of BPD secondary to preeclampsia and the therapeutic pathways targeted by vitamin D may help identify precise therapies to mitigate the growing burden of BPD.

DATA AVAILABILITY

The datasets generated during and/or analyzed during the current study are available from the corresponding author upon reasonable request.

ACKNOWLEDGMENTS

Graphical abstract created with a licensed version of BioRender.

GRANTS

This work was supported in part by the National Heart, Lung, and Blood Institute (NHLBI) Grant T32 HL160508 and the APP Marshall Klaus Award in Basic Science (to M.W.C.); Grants K08 HL150222 and UL1 TR002535 (to E.W.M.); Grant R01 HL151630 (to B.J.S.).

DISCLOSURES

No conflicts of interest, financial or otherwise, are declared by the authors.

AUTHOR CONTRIBUTIONS

M.W.C. and E.W.M. conceived and designed research; M.W.C., T.G., E.M.B., G.S., and S.E. performed experiments; M.W.C., T.G., E.M.B., and G.S. analyzed data; M.W.C., T.G., E.M.B., B.J.S., and E.W.M. interpreted results of experiments; M.W.C. prepared figures; M.W.C. drafted manuscript; M.W.C., T.G., E.M.B., G.S., B.J.S., J.C.F., and E.W.M. edited and revised manuscript; M.W.C., T.G., E.M.B., G.S., B.J.S., J.C.F., and E.W.M. approved final version of manuscript.

REFERENCES

1. **Jobe AH**, **Bancalari E.** Bronchopulmonary dysplasia. *Am J Respir Crit Care Med* 163: 1723–1729, 2001. doi:10.1164/ajrccm.163.7.2011060.
2. **Baraldi E**, **Filippone M.** Chronic lung disease after premature birth. *N Engl J Med* 357: 1946–1955, 2007. doi:10.1056/NEJMra067279.
3. **Kinsella JP**, **Greenough A**, **Abman SH.** Bronchopulmonary dysplasia. *Lancet* 367: 1421–1431, 2006. doi:10.1016/S0140-6736(06)68615-7.
4. **Thébaud B**, **Goss KN**, **Laughon M**, **Whitsett JA**, **Abman SH**, **Steinhorn RH**, **Aschner JL**, **Davis PG**, **McGrath-Morrow SA**, **Soll RF**, **Jobe AH.** Bronchopulmonary dysplasia. *Nat Rev Dis Primers* 5: 78, 2019. doi:10.1038/s41572-019-0127-7.
5. **Bell EF**, **Hintz SR**, **Hansen NI**, **Bann CM**, **Wyckoff MH**, **DeMauro SB**, **Walsh MC**, **Vohr BR**, **Stoll BJ**, **Carlo WA**, **Van Meurs KP**, **Rysavy MA**, **Patel RM**, **Merhar SL**, **Sánchez PJ**, **Laptook AR**, **Hibbs AM**, **Cotten CM**, **D'Angio CT**, **Winter S**, **Fuller J**, **Das A**; **Eunice Kennedy Shriver National Institute of Child Health and Human Development Neonatal Research Network.** Mortality, in-hospital morbidity, care practices, and 2-year outcomes for extremely preterm infants in the US, 2013-2018. *JAMA* 327: 248–263, 2022. doi:10.1001/jama.2021.23580.
6. **Jensen EA**, **Edwards EM**, **Greenberg LT**, **Soll RF**, **Ehret DEY**, **Horbar JD.** Severity of bronchopulmonary dysplasia among very preterm infants in the United States. *Pediatrics* 148: e2020030007, 2021. doi:10.1542/peds.2020-030007.
7. **Jensen EA**, **Dysart K**, **Gantz MG**, **McDonald S**, **Bamat NA**, **Keszler M**, **Kirpalani H**, **Laughon MM**, **Poindexter BB**, **Duncan AF**, **Yoder BA**, **Eichenwald EC**, **DeMauro SB.** The diagnosis of bronchopulmonary dysplasia in very preterm infants. An evidence-based approach. *Am J Respir Crit Care Med* 200: 751–759, 2019. doi:10.1164/rccm.201812-2348OC.
8. **Northway WH Jr**, **Rosan RC**, **Porter DY.** Pulmonary disease following respirator therapy of hyaline-membrane disease. Bronchopulmonary dysplasia. *N Engl J Med* 276: 357–368, 1967. doi:10.1056/NEJM196702162760701.
9. **Schmidt B**, **Roberts RS**, **Davis PG**, **Doyle LW**, **Asztalos EV**, **Opie G**, **Bairam A**, **Solimano A**, **Arnon S**, **Sauve RS**; **Caffeine for Apnea of Prematurity (CAP) Trial Investigators, Caffeine for Apnea of Prematurity CAP Trial Investigators.** Prediction of late death or disability at age 5 years using a count of 3 neonatal morbidities in very low birth weight infants. *J Pediatr* 167: 982–986.e2, 2015. doi:10.1016/j.jpeds.2015.07.067.
10. **Arjaans S**, **Haarman MG**, **Roofthooft MTR**, **Fries MWF**, **Kooi EMW**, **Bos AF**, **Berger RMF.** Fate of pulmonary hypertension associated with bronchopulmonary dysplasia beyond 36 weeks postmenstrual age. *Arch Dis Child Fetal Neonatal Ed* 106: 45–50, 2021. doi:10.1136/archdischild-2019-318531.
11. **Thébaud B**, **Abman SH.** Bronchopulmonary dysplasia: where have all the vessels gone? Roles of angiogenic growth factors in chronic lung disease. *Am J Respir Crit Care Med* 175: 978–985, 2007. doi:10.1164/rccm.200611-1660PP.
12. **Abman SH.** Bronchopulmonary dysplasia: "a vascular hypothesis". *Am J Respir Crit Care Med* 164: 1755–1756, 2001. doi:10.1164/ajrccm.164.10.2109111c.
13. **Jakkula M**, **Le Cras TD**, **Gebb S**, **Hirth KP**, **Tuder RM**, **Voelkel NF**, **Abman SH.** Inhibition of angiogenesis decreases alveolarization in the developing rat lung. *Am J Physiol Lung Cell Mol Physiol* 279: L600–L607, 2000. doi:10.1152/ajplung.2000.279.3.L600.
14. **Le Cras TD**, **Markham NE**, **Tuder RM**, **Voelkel NF**, **Abman SH.** Treatment of newborn rats with a VEGF receptor inhibitor causes pulmonary hypertension and abnormal lung structure. *Am J Physiol Lung Cell Mol Physiol* 283: L555–L562, 2002. doi:10.1152/ajplung.00408.2001.
15. **Bhatt AJ**, **Pryhuber GS**, **Huyck H**, **Watkins RH**, **Metlay LA**, **Maniscalco WM.** Disrupted pulmonary vasculature and decreased vascular endothelial growth factor, Flt-1, and TIE-2 in human infants dying with bronchopulmonary dysplasia. *Am J Respir Crit Care Med* 164: 1971–1980, 2001. doi:10.1164/ajrccm.164.10.2101140.
16. **Stojanovska V**, **Scherjon SA**, **Plösch T.** Preeclampsia as modulator of offspring health. *Biol Reprod* 94: 53, 2016. doi:10.1095/biolreprod.115.135780.
17. **Staff AC**, **Braekke K**, **Harsem NK**, **Lyberg T**, **Holthe MR.** Circulating concentrations of sFlt1 (soluble fms-like tyrosine kinase 1) in fetal and maternal serum during pre-eclampsia. *Eur J Obstet Gynecol Reprod Biol* 122: 33–39, 2005. doi:10.1016/j.ejogrb.2004.11.015.
18. **Vuorela P**, **Helske S**, **Hornig C**, **Alitalo K**, **Weich H**, **Halmesmäki E.** Amniotic fluid–soluble vascular endothelial growth factor receptor-1 in preeclampsia. *Obstet Gynecol* 95: 353–357, 2000. doi:10.1016/s0029-7844(99)00565-7.
19. **Hansen AR**, **Barnés CM**, **Folkman J**, **Mcelrath TF.** Maternal preeclampsia predicts the development of bronchopulmonary dysplasia. *J Pediatr* 156: 532–536, 2010. doi:10.1016/j.jpeds.2009.10.018.
20. **Tagliaferro T**, **Jain D**, **Vanbuskirk S**, **Bancalari E**, **Claure N.** Maternal preeclampsia and respiratory outcomes in extremely premature infants. *Pediatr Res* 85: 693–696, 2019. doi:10.1038/s41390-019-0336-5.
21. **Morrow LA**, **Wagner BD**, **Ingram DA**, **Poindexter BB**, **Schibler K**, **Cotten CM**, **Dagle J**, **Sontag MK**, **Mourani PM**, **Abman SH.** Antenatal determinants of bronchopulmonary dysplasia and late respiratory disease in preterm infants. *Am J Respir Crit Care Med* 196: 364–374, 2017. doi:10.1164/rccm.201612-2414OC.
22. **Pierro M**, **Villamor-Martinez E**, **Van Westering-Kroon E**, **Alvarez-Fuente M**, **Abman SH**, **Villamor E.** Association of the dysfunctional placentation endotype of prematurity with bronchopulmonary dysplasia: a systematic review, meta-analysis and meta-regression. *Thorax* 77: 268–275, 2022. doi:10.1136/thoraxjnl-2020-216485.
23. **Mestan KK**, **Check J**, **Minturn L**, **Yallapragada S**, **Farrow KN**, **Liu X**, **Su E**, **Porta N**, **Gotteiner N**, **Ernst LM.** Placental pathologic changes of maternal vascular underperfusion in bronchopulmonary dysplasia and pulmonary hypertension. *Placenta* 35: 570–574, 2014. doi:10.1016/j.placenta.2014.05.003.
24. **Mestan KK**, **Gotteiner N**, **Porta N**, **Grobman W**, **Su EJ**, **Ernst LM.** Cord blood biomarkers of placental maternal vascular underperfusion predict bronchopulmonary dysplasia-associated pulmonary hypertension. *J Pediatr* 185: 33–41, 2017. doi:10.1016/j.jpeds.2017.01.015.
25. **Zeisler H**, **Llurba E**, **Chantraine F**, **Vatish M**, **Staff AC**, **Sennström M**, **Olovsson M**, **Brennecke SP**, **Stepan H**, **Allegranza D**, **Dilba P**, **Schoedl M**, **Hund M**, **Verlohren S.** Predictive value of the sFlt-1: PLGF ratio in women with suspected preeclampsia. *N Engl J Med* 374: 13–22, 2016. doi:10.1056/NEJMoa1414838.
26. **Wang CN**, **Chang SD**, **Peng HH**, **Lee YS**, **Chang YL**, **Cheng PJ**, **Chao AS**, **Wang TH**, **Wang HS.** Change in amniotic fluid levels of multiple anti-angiogenic proteins before development of preeclampsia and intrauterine growth restriction. *J Clin Endocrinol Metab* 95: 1431–1441, 2010. doi:10.1210/jc.2009-1954.
27. **Hasan J**, **Beharry KD**, **Valencia AM**, **Strauss A**, **Modanlou HD.** Soluble vascular endothelial growth factor receptor 1 in tracheal aspirate fluid of preterm neonates at birth may be predictive of bronchopulmonary dysplasia/chronic lung disease. *Pediatrics* 123: 1541–1547, 2009. doi:10.1542/peds.2008-1670.
28. **Wallace B**, **Peisl A**, **Seedorf G**, **Nowlin T**, **Kim C**, **Bosco J**, **Kenniston J**, **Keefe D**, **Abman SH.** Anti–sFlt-1 therapy preserves lung alveolar and vascular growth in antenatal models of bronchopulmonary dysplasia. *Am J Respir Crit Care Med* 197: 776–787, 2018. doi:10.1164/rccm.201707-1371OC.
29. **Tang JR**, **Karumanchi SA**, **Seedorf G**, **Markham N**, **Abman SH.** Excess soluble vascular endothelial growth factor receptor-1 in amniotic fluid impairs lung growth in rats: linking preeclampsia with bronchopulmonary dysplasia. *Am J Physiol Lung Cell Mol Physiol* 302: L36–L46, 2012. doi:10.1152/ajplung.00294.2011.
30. **Christakos S**, **Li S**, **De La Cruz J**, **Bikle DD.** New developments in our understanding of vitamin metabolism, action and treatment. *Metabolism* 98: 112–120, 2019. doi:10.1016/j.metabol.2019.06.010.
31. **Norman AW.** Vitamin D receptor: new assignments for an already busy receptor. *Endocrinology* 147: 5542–5548, 2006. doi:10.1210/en.2006-0946.
32. **Mandell E**, **Seedorf GJ**, **Ryan S**, **Gien J**, **Cramer SD**, **Abman SH.** Antenatal endotoxin disrupts lung vitamin D receptor and 25-hydroxyvitamin D 1α-hydroxylase expression in the developing rat. *Am J Physiol Lung Cell Mol Physiol* 309: L1018–L1026, 2015. doi:10.1152/ajplung.00253.2015.
33. **Nguyen M**, **Trubert CL**, **Rizk-Rabin M**, **Rehan VK**, **Besançon F**, **Cayre YE**, **Garabédian M.** 1,25-Dihydroxyvitamin D3 and fetal lung maturation: immunogold detection of VDR expression in pneumocytes type II cells and effect on fructose 1,6 bisphosphatase. *J Steroid Biochem Mol Biol* 89-90: 93–97, 2004. doi:10.1016/j.jsbmb.2004.03.054.
34. **Nguyen TM**, **Guillozo H**, **Marin L**, **Dufour ME**, **Tordet C**, **Pike JW**, **Garabedian M.** 1,25-dihydroxyvitamin D3 receptors in rat lung

during the perinatal period: regulation and immunohistochemical localization. *Endocrinology* 127: 1755–1762, 1990. doi:10.1210/endo-127-4-1755.

35. **Nguyen M**, **Guillozo H**, **Garabédian M**, **Balsan S.** Lung as a possible additional target organ for vitamin D during fetal life in the rat. *Biol Neonate* 52: 232–240, 1987. doi:10.1159/000242714.
36. **Merke J**, **Milde P**, **Lewicka S**, **Hügel U**, **Klaus G**, **Mangelsdorf DJ**, **Haussler MR**, **Rauterberg EW**, **Ritz E.** Identification and regulation of 1,25-dihydroxyvitamin D3 receptor activity and biosynthesis of 1,25-dihydroxyvitamin D3. Studies in cultured bovine aortic endothelial cells and human dermal capillaries. *J Clin Invest* 83: 1903–1915, 1989. doi:10.1172/JCI114097.
37. **Sakurai R**, **Singh H**, **Wang Y**, **Harb A**, **Gornes C**, **Liu J**, **Rehan VK.** Effect of perinatal vitamin D deficiency on lung mesenchymal stem cell differentiation and injury repair potential. *Am J Respir Cell Mol Biol* 65: 521–531, 2021. doi:10.1165/rcmb.2020-0183OC.
38. **Sakurai R**, **Shin E**, **Fonseca S**, **Sakurai T**, **Litonjua AA**, **Weiss ST**, **Torday JS**, **Rehan VK.** 1alpha,25$(OH)_2D_3$ and its 3-epimer promote rat lung alveolar epithelial-mesenchymal interactions and inhibit lipofibroblast apoptosis. *Am J Physiol Lung Cell Mol Physiol* 297: L496–L505, 2009. doi:10.1152/ajplung.90539.2008.
39. **Nguyen TM**, **Guillozo H**, **Marin L**, **Tordet C**, **Koite S**, **Garabedian M.** Evidence for a vitamin D paracrine system regulating maturation of developing rat lung epithelium. *Am J Physiol Lung Cell Mol Physiol* 271: L392–L399, 1996. doi:10.1152/ajplung.1996.271.3.L392.
40. **Marin L**, **Dufour ME**, **Nguyen TM**, **Tordet C**, **Garabedian M.** Maturational changes induced by 1 alpha,25-dihydroxyvitamin D3 in type II cells from fetal rat lung explants. *Am J Physiol Lung Cell Mol Physiol* 265: L45–L52, 1993. doi:10.1152/ajplung.1993.265.1.L45.
41. **Wang Y**, **Jiang L.** Role of vitamin D–vitamin D receptor signaling on hyperoxia-induced bronchopulmonary dysplasia in neonatal rats. *Pediatr Pulmonol* 56: 2335–2344, 2021. doi:10.1002/ppul.25418.
42. **Mandell E**, **Seedorf G**, **Gien J**, **Abman SH.** Vitamin D treatment improves survival and infant lung structure after intra-amniotic endotoxin exposure in rats: potential role for the prevention of bronchopulmonary dysplasia. *Am J Physiol Lung Cell Mol Physiol* 306: L420–L428, 2014. doi:10.1152/ajplung.00344.2013.
43. **Cookson MW**, **Ryan SL**, **Seedorf GJ**, **Dodson RB**, **Abman SH**, **Mandell EW.** Antenatal vitamin D preserves placental vascular and fetal growth in experimental chorioamnionitis due to intra-amniotic endotoxin exposure. *Am J Perinatol* 35: 1260–1270, 2018. doi:10.1055/s-0038-1642033.
44. **Mandell E**, **Powers KN**, **Harral JW**, **Seedorf GJ**, **Hunter KS**, **Abman SH**, **Dodson RB.** Intrauterine endotoxin-induced impairs pulmonary vascular function and right ventricular performance in infant rats and improvement with early vitamin D therapy. *Am J Physiol Lung Cell Mol Physiol* 309: L1438–L1446, 2015. doi:10.1152/ajplung.00302.2015.
45. **Cooney TP**, **Thurlbeck WM.** The radial alveolar count method of Emery and Mithal: a reappraisal 1–postnatal lung growth. *Thorax* 37: 572–579, 1982. doi:10.1136/thx.37.8.572.
46. **Emery JL**, **Mithal A.** The number of alveoli in the terminal respiratory unit of man during late intrauterine life and childhood. *Arch Dis Child* 35: 544–547, 1960. doi:10.1136/adc.35.184.544.
47. **Hsia CC**, **Hyde DM**, **Ochs M**, **Weibel ER**; **ATS/ERS Joint Task Force on Quantitative Assessment of Lung Structure.** An official research policy statement of the American Thoracic Society/European Respiratory Society: standards for quantitative assessment of lung structure. *Am J Respir Crit Care Med* 181: 394–418, 2010. doi:10.1164/rccm.200809-1522ST.
48. **Alphonse RS**, **Vadivel A**, **Zhong S**, **Mcconaghy S**, **Ohls R**, **Yoder MC**, **Thébaud B.** The isolation and culture of endothelial colony-forming cells from human and rat lungs. *Nat Protoc* 10: 1697–1708, 2015 [Erratum in *Nat Protoc* 111: 192, 2016]. doi:10.1038/nprot.2015.107.
49. **Gien J**, **Seedorf GJ**, **Balasubramaniam V**, **Tseng N**, **Markham N**, **Abman SH.** Chronic intrauterine pulmonary hypertension increases endothelial cell Rho kinase activity and impairs angiogenesis in vitro. *Am J Physiol Lung Cell Mol Physiol* 295: L680–L687, 2008. doi:10.1152/ajplung.00516.2007.
50. **McGrath-Morrow SA**, **Cho C**, **Cho C**, **Zhen L**, **Hicklin DJ**, **Tuder RM.** Vascular endothelial growth factor receptor 2 blockade disrupts postnatal lung development. *Am J Respir Cell Mol Biol* 32: 420–427, 2005. doi:10.1165/rcmb.2004-0287OC.
51. **Seedorf G**, **Kim C**, **Wallace B**, **Mandell EW**, **Nowlin T**, **Shepherd D**, **Abman SH.** rhIGF-1/BP3 preserves lung growth and prevents pulmonary hypertension in experimental bronchopulmonary dysplasia. *Am J Respir Crit Care Med* 201: 1120–1134, 2020. doi:10.1164/rccm.201910-1975OC.
52. **Yun EJ**, **Lorizio W**, **Seedorf G**, **Abman SH**, **Vu TH.** VEGF and endothelium-derived retinoic acid regulate lung vascular and alveolar development. *Am J Physiol Lung Cell Mol Physiol* 310: L287–L298, 2016. doi:10.1152/ajplung.00229.2015.
53. **Seedorf G**, **Metoxen AJ**, **Rock R**, **Markham N**, **Ryan S**, **Vu T**, **Abman SH.** Hepatocyte growth factor as a downstream mediator of vascular endothelial growth factor-dependent preservation of growth in the developing lung. *Am J Physiol Lung Cell Mol Physiol* 310: L1098–L1110, 2016. doi:10.1152/ajplung.00423.2015.
54. **Vila Ellis L**, **Cain MP**, **Hutchison V**, **Flodby P**, **Crandall ED**, **Borok Z**, **Zhou B**, **Ostrin EJ**, **Wythe JD**, **Chen J.** Epithelial Vegfa specifies a distinct endothelial population in the mouse lung. *Dev Cell* 52: 617–630.e6, 2020. doi:10.1016/j.devcel.2020.01.009.
55. **Mourani PM**, **Sontag MK**, **Younoszai A**, **Miller JI**, **Kinsella JP**, **Baker CD**, **Poindexter BB**, **Ingram DA**, **Abman SH.** Early pulmonary vascular disease in preterm infants at risk for bronchopulmonary dysplasia. *Am J Respir Crit Care Med* 191: 87–95, 2015. doi:10.1164/rccm.201409-1594OC.
56. **Goss KN**, **Beshish AG**, **Barton GP**, **Haraldsdottir K**, **Levin TS**, **Tetri LH**, **Battiola TJ**, **Mulchrone AM**, **Pegelow DF**, **Palta M**, **Lamers LJ**, **Watson AM**, **Chesler NC**, **Eldridge MW.** Early pulmonary vascular disease in young adults born preterm. *Am J Respir Crit Care Med* 198: 1549–1558, 2018. doi:10.1164/rccm.201710-2016OC.
57. **Zanini F**, **Che X**, **Knutsen C**, **Liu M**, **Suresh NE**, **Domingo-Gonzalez R**, **Dou SH**, **Zhang D**, **Pryhuber GS**, **Jones RC**, **Quake SR**, **Cornfield DN**, **Alvira CM.** Developmental diversity and unique sensitivity to injury of lung endothelial subtypes during postnatal growth. *iScience* 26: 106097, 2023. doi:10.1016/j.isci.2023.106097.
58. **Schupp JC**, **Adams TS**, **Cosme C**, **Raredon MSB**, **Yuan Y**, **Omote N**, **Poli S**, **Chioccioli M**, **Rose K-A**, **Manning EP**, **Sauler M**, **Deluliis G**, **Ahangari F**, **Neumark N**, **Habermann AC**, **Gutierrez AJ**, **Bui LT**, **Lafyatis R**, **Pierce RW**, **Meyer KB**, **Nawijn MC**, **Teichmann SA**, **Banovich NE**, **Kropski JA**, **Niklason LE**, **Pe'er D**, **Yan X**, **Homer RJ**, **Rosas IO**, **Kaminski N.** Integrated single-cell atlas of endothelial cells of the human lung. *Circulation* 144: 286–302, 2021. doi:10.1161/CIRCULATIONAHA.120.052318.
59. **Rodor J**, **Chen SH**, **Scanlon JP**, **Monteiro JP**, **Caudrillier A**, **Sweta S**, **Stewart KR**, **Shmakova A**, **Dobie R**, **Henderson BEP**, **Stewart K**, **Hadoke PWF**, **Southwood M**, **Moore SD**, **Upton PD**, **Morrell NW**, **Li Z**, **Chan SY**, **Handen A**, **Lafyatis R**, **De Rooij LPMH**, **Henderson NC**, **Carmeliet P**, **Spiroski AM**, **Brittan M**, **Baker AH.** Single-cell RNA sequencing profiling of mouse endothelial cells in response to pulmonary arterial hypertension. *Cardiovasc Res* 118: 2519–2534, 2022. doi:10.1093/cvr/cvab296.
60. **Guo M**, **Du Y**, **Gokey JJ**, **Ray S**, **Bell SM**, **Adam M**, **Sudha P**, **Perl AK**, **Deshmukh H**, **Potter SS**, **Whitsett JA**, **Xu Y.** Single cell RNA analysis identifies cellular heterogeneity and adaptive responses of the lung at birth. *Nat Commun* 10: 37, 2019. doi:10.1038/s41467-018-07770-1.
61. **Liu NQ**, **Hewison M.** Vitamin D, the placenta and pregnancy. *Arch Biochem Biophys* 523: 37–47, 2012. doi:10.1016/j.abb.2011.11.018.
62. **Olmos-Ortiz A**, **Avila E**, **Durand-Carbajal M**, **Díaz L.** Regulation of calcitriol biosynthesis and activity: focus on gestational vitamin D deficiency and adverse pregnancy outcomes. *Nutrients* 7: 443–480, 2015. doi:10.3390/nu7010443.
63. **Kose M**, **Bastug O**, **Sonmez MF**, **Per S**, **Ozdemir A**, **Kaymak E**, **Yahşi H**, **Ozturk MA.** Protective effect of vitamin D against hyperoxia-induced lung injury in newborn rats. *Pediatr Pulmonol* 52: 69–76, 2017. doi:10.1002/ppul.23500.
64. **Yao L**, **Shi Y**, **Zhao X**, **Hou A**, **Xing Y**, **Fu J**, **Xue X.** Vitamin D attenuates hyperoxia-induced lung injury through downregulation of Toll-like receptor 4. *Int J Mol Med* 39: 1403–1408, 2017. doi:10.3892/ijmm.2017.2961.
65. **Chen C**, **Weng H**, **Zhang X**, **Wang S**, **Lu C**, **Jin H**, **Chen S**, **Liu Y**, **Sheng A**, **Sun Y.** Low-dose vitamin d protects hyperoxia-induced bronchopulmonary dysplasia by inhibiting neutrophil extracellular traps. *Front Pediatr* 8: 335, 2020. doi:10.3389/fped.2020.00335.
66. **Hu J**, **Wu Z**, **Wang H**, **Geng H**, **Huo J**, **Zhu X**, **Zhu X.** Vitamin D ameliorates apoptosis and inflammation by targeting the mitochondrial and MEK1/2-ERK1/2 pathways in hyperoxia-induced bronchopulmonary dysplasia. *J Inflamm Res* 15: 4891–4906, 2022. doi:10.2147/JIR.S371906.